20.8 A Dual-Frequency 0.7-to-1GHz Balance Network for Electrical Balance Duplexers

Benjamin Hershberg[1], Barend van Liempd[1,2], Xiaoqiang Zhang[1], Piet Wambacq[1,2], Jan Craninckx[1]

[1]imec, Heverlee, Belgium, [2]Vrije Universiteit Brussel, Brussels, Belgium

An electrical-balance duplexer (EBD) is a tunable RF front-end concept that seeks to address several key challenges of 4G and 5G mobile systems [1]. The basic principle is shown in Fig. 20.8.1. Duplexer isolation is achieved when the signals in paths 1 and 2 cancel and prevent the TX signal from appearing at the RX port. This cancellation is achieved by "balancing" the antenna impedance Z_{ANT} with an on-chip tunable impedance Z_{BAL}.

In frequency-division duplex (FDD) mobile applications, Z_{BAL} is the most challenging and critical sub-block in an EBD design. FDD TX and RX channels are always at separate frequencies, and Z_{BAL} must be able to balance the antenna at both, simultaneously. Moreover, the antenna impedance varies over time due to user interaction, and must be tracked by the balance network.

Previous EBD works report large isolation bandwidths, often spanning across both the TX and RX channels. This seems to suggest that dual-frequency tuning has already been solved. But these claims are highly misleading for two reasons. First, the isolation bandwidth is determined by both the impedance profile of Z_{BAL} *and* the antenna. If the impedance used for Z_{ANT} is not realistic (e.g. a fixed 50Ω) then the measured isolation bandwidth is meaningless. Second, it is the worst-case scenario that we are most interested in knowing, not the best-case. The antenna impedance varies due to user interaction, and Z_{BAL} must be able to synthesize a balancing impedance for *any* possible scenario within this range of variability. It is not sufficient to generate a large range of impedances at TX and RX frequencies. One must be able to generate any TX impedance simultaneously with any RX impedance. To date, there is no work that has taken these two considerations into account, and, as a result, the tuning range and isolation bandwidths reported often say very little about practical performance. Although several works demonstrate dual-frequency balancing for selective cases [2,3], none do so in a way that is general enough to actually solve the problem. In this paper, we present one such FDD-capable balance network, compliant with all LTE bands in the 0.7-to-1GHz range.

Figure 20.8.2 introduces an approach that addresses the key challenges mentioned above. The main idea is to have a portion of the network that only influences the impedance at one frequency. This is accomplished by using an allpass tunable front-end impedance block, followed by a narrowband filter and terminated with a variable-bandwidth back-end block. If the filter is configured to have a passband at f_1 and stopband at f_2, tuning the back-end block only influences the network input impedance at f_1. By contrast, adjusting the front-end of the network influences the impedance at f_1 and f_2. The benefit of this is two-fold. For one, it makes full coverage possible, since each $Z_{BAL}(f_2)$ that can be synthesized by the front-end is associated with an entire range of $Z_{BAL}(f_1)$ that can be synthesized with the back-end. Second, it dramatically reduces the tuning complexity, since we can first synthesize $Z_{BAL}(f_2)$ using the front-end control knobs and then independently synthesize $Z_{BAL}(f_1)$ with the back-end knobs.

Figure 20.8.3 provides two specifications that can be used to describe the "full coverage" dual-frequency tuning capability of an EBD (or Z_{BAL} alone). Region$_{TX}$ specifies the impedance region in which the network can synthesize *any* impedance at f_{TX}. Region$_{RX}$ specifies the area around *any* $Z_{BAL}(f_{TX})$ within region$_{TX}$ for which *any* impedance at f_{RX} can be synthesized concurrently. We choose this criteria because the antenna impedance is expected to change (w.r.t. frequency) on the complex plane from $Z_{ANT}(f_{TX})$ to $Z_{ANT}(f_{RX})$ in an unknown trajectory and at some unknown rate of change that is limited by the Q of the antenna. Region$_{RX}$ thus relates the balance-network tuning capabilities to the maximum antenna Q that it can reliably operate with. This rate of change relative to $Z_{ANT}(f_{TX})$, given in %/MHz (chosen w.r.t. some f_{ref}), describes the underlying behavior of the system irrespective of the specific TX/RX channel spacing, allowing a single specification to be used for many bands.

In Fig. 20.8.4 we present an LC-ladder topology that implements the concept of Fig. 20.8.2. Due to the broad range of supported frequencies that we target and the limited Q of actual components, we find that the three conceptual blocks are most efficiently implemented in a distributed manner. Rather than having a dedicated filter block, the filtering gradually accumulates with each successive ladder stage in the network. To ensure that the filtering provides a consistent pass/stop characteristic, the component values in the front stages of the network are chosen such that all resonances are above 1GHz. This guarantees that the filtering action is always lowpass in nature in the 0.7-to-1GHz range for any possible setting. By contrast, the component values of the back-end stages are chosen such that in-band resonances can occur for some network settings but lie out-of-band for others. This is critical for generating full coverage.

Determining the required degrees of freedom and the appropriate component values for the network is non-trivial. At the core of the effort lies a unique simulation tool that we have built for the task. Unlike conventional simulators, it describes the circuit as a hierarchy of closed-form symbolic n-port equations. With such an equation describing Z_{BAL}, we can rapidly simulate billions of different network settings in a matter of hours. This brute-force approach allows us to both quickly visualize the tuning capabilities of the network during design and fully validate it prior to fabrication.

The frequency-dependent tuning range of the network (region$_{RX}$) is maximized by maximizing the overall Q of the network. Yet, we wish to synthesize impedances in the vicinity of 50Ω. These opposing goals are satisfied by using a large number of high-Q reactive components in the network, which, in total, contain enough distributed parasitic resistance to synthesize 50Ω. The digitally tuned capacitors of the network are comprised of banks of a unit-capacitor structure C_U, depicted in Fig. 20.8.4. In order to withstand large voltages that are present in the EBD under full-power operation, six SOI NMOS transistors are stacked to form each switch. Additional drain-source MIM capacitors are added to improve the equalization of AC voltages across the stack, at the cost of slightly reduced C_{ON}/C_{OFF} ratio.

The balance network is fabricated in a 0.18μm RF SOI CMOS technology, with an active area of 8.28mm^2. For all measurements, the de-embedded reference plane lies at the input pads (see die micrograph of Fig. 20.8.7). Figure 20.8.6 summarizes the performance, valid for all 10 LTE bands in the 0.7-to-1GHz range. Validation is conducted by iteratively programming 1.85 million random network configurations into the chip and analyzing the resulting S_{11} dataset. For this design, a 1.1:1 VSWR region is chosen for region$_{TX}$ based on the assumption that there is an antenna tuner available that is capable of this level of accuracy (Fig. 20.8.1). While a much larger region$_{TX}$ VSWR is available, as shown in Fig. 20.8.6, it comes with a trade-off in the size/shape of region$_{RX}$. Four noteworthy region$_{RX}$ visualizations are plotted in Fig. 20.8.5. The black circles represent the region$_{RX}$ boundary. Figure 20.8.5a is LTE band 5, and Fig. 20.8.5b is an inverted LTE band 5 with f_{TX} and f_{RX} swapped. This comparison demonstrates that a similar tuning coverage occurs for either ordering of f_{TX} and f_{RX}. Figure 20.8.5c is LTE band 14 (30MHz TX/RX band spacing) and Fig. 20.8.5d shows the impedance characteristics when the TX/RX spacing is increased to 100MHz for a non-standard band. This demonstrates that the network generates fully filled region$_{RX}$ areas that scale in diameter relative to both the TX/RX channel spacing and absolute frequency location.

A custom tuning algorithm that exploits the network orthogonal-tuning functionality has been implemented. It is systematically tested across the entire region$_{TX}$ and region$_{RX}$ areas for all 10 LTE bands. The algorithm finds a solution with ≥40dB matching (at both f_{TX} and f_{RX}) in 479 trials on average, with $\sigma = 605$, median = 259, and max = 4304. This accuracy is only limited by the finite resolution of the tunable capacitors and can easily be improved in future designs. The only input to the algorithm is the magnitude of impedance balancing at f_{TX} and f_{RX}.

This work provides a solution to the essential EBD challenge of dual-frequency impedance balancing and tracking. When integrated into an EBD, it enables reliable FDD duplexing with actual antennas in real world environments.

Acknowledgement:
This work is part of imec's green radio program and is partly sponsored by HiSilicon, Panasonic, Murata, GlobalFoundries and Cadence.

References:
[1] M. Mikhemar et al., "A Tunable Integrated Duplexer with 50dB Isolation in 40nm CMOS," *ISSCC Dig. Tech. Papers*, pp. 386-387, Feb. 2009.
[2] S. Abdelhalem et al., "Tunable CMOS Integrated Duplexer With Antenna Impedance Tracking and High Isolation in the Transmit and Receive Bands," *IEEE Trans. on Microwave Theory and Techniques*, vol. 62, no. 9, pp. 2092-2104, Sept. 2014.
[3] B. van Liempd et al., "A Dual-Notch +27dBm TX-Power Electrical-Balance Duplexer," *European Solid State Circuits Conference,* pp.463-466, Sept. 2014.

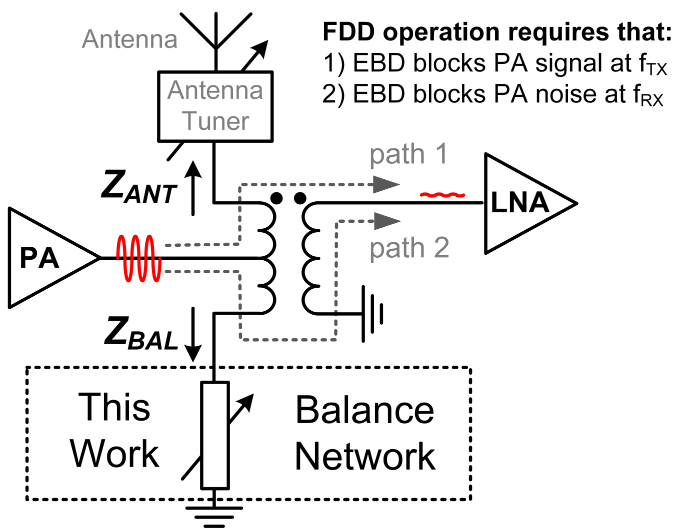

Figure 20.8.1: Tunable electrical-balance duplexer (EBD).

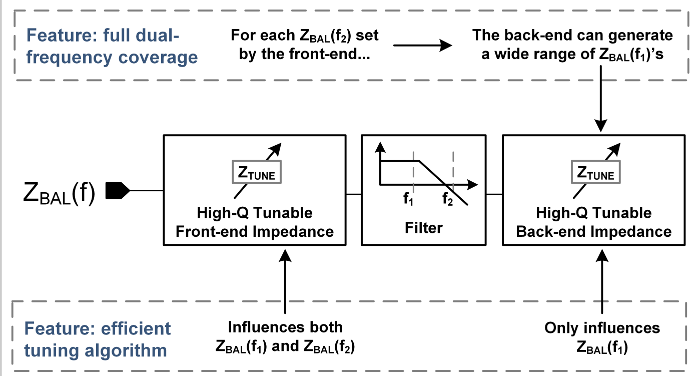

Figure 20.8.2: Dual-frequency impedance-synthesis concept.

For any $Z_{ANT}(f_{TX})$ being balanced within $region_{TX}$, the network must simultaneously balance any $Z_{ANT}(f_{RX})$ within $region_{RX}$

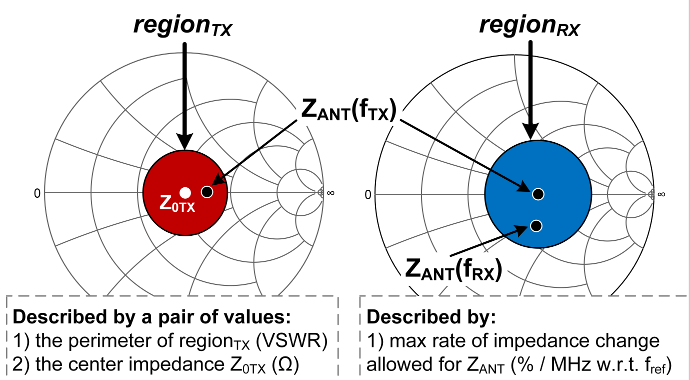

The spec for $region_{RX}$ (% / MHz) is related to the $region_{RX}$ perimeter as:

$$region_{RX}\ perimeter = \frac{Z_{ANT}(f_{TX}) \cdot \left[region_{RX} \cdot |f_{TX} - f_{RX}| \cdot (f_{TX} + f_{RX})(1 + e^{j\phi}) + f_{ref} \cdot 4 \times 10^{8}\right]}{region_{RX} \cdot |f_{TX} - f_{RX}| \cdot (f_{TX} + f_{RX})(1 - e^{j\phi}) + f_{ref} \cdot 4 \times 10^{8}}$$

Figure 20.8.3: Specifications for describing dual-frequency coverage.

Dual-Frequency Balance Network Topology (Z_{BAL})

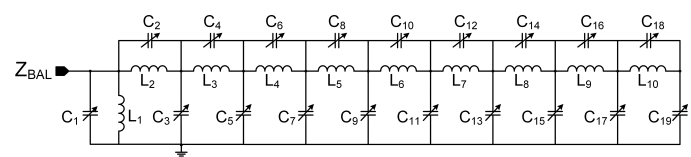

Component Values

Name	Value	Q (0.7-1GHz)
L_1	18.2nH	Q > 12
L_2	9.1nH	Q > 15
L_3-L_{10}	11.1nH	Q > 15
C_U	C_{ON} = 117fF C_{OFF} = 33fF	Q_{ON} > 25 Q_{OFF} > 10
C_1, C_3, C_5, C_7, C_9, C_{11}	40 x C_U	-
C_2, C_4, C_6, C_8, C_{10}	28 x C_U	-
C_{12} - C_{19}	48 x C_U	-

C_U Unit Capacitor Circuit

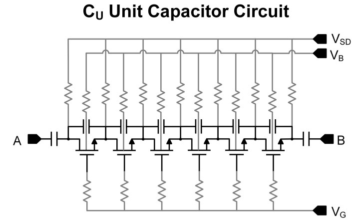

Figure 20.8.4: Balance network topology and design details.

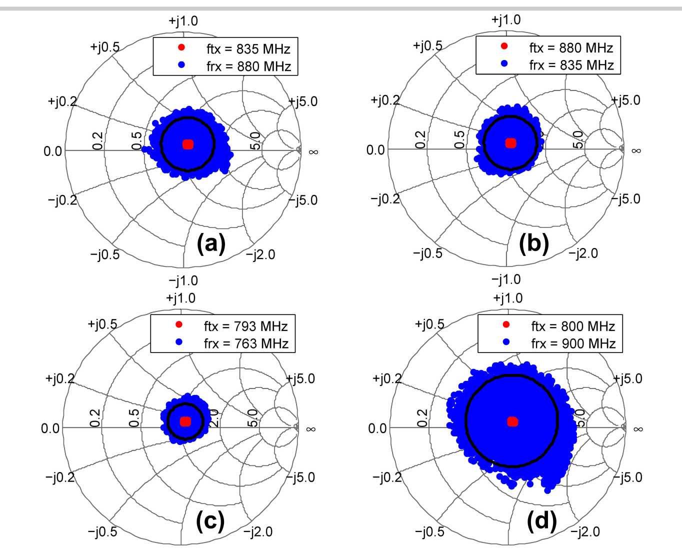

Figure 20.8.5: Dual-frequency tuning range ($region_{RX}$) for 4 cases.

Measured Dual-Frequency Tuning Performance

Technology	0.18μm RF SOI CMOS
Chip Area	8.28mm^2 (3.6mm x 2.3mm)
Operating Range	0.7GHz – 1.0GHz
$Region_{TX}$	1.1:1 VSWR, 54+j5Ω
$Region_{RX}$	1.2%/MHz (w.r.t. 800MHz)
LTE Bands Validated	5, 6, 8, 12, 13, 14, 17, 18, 19, 20
Impedance match*	> 40dB
Isolation Bandwidth	N/A (requires antenna)
Tuning efficiency**	mean = 479 measurements σ = 605 measurements max = 4304 measurements

*this value is different from (but closely related to) duplexer isolation
**based on testing across complete tuning regions of 10 LTE bands.

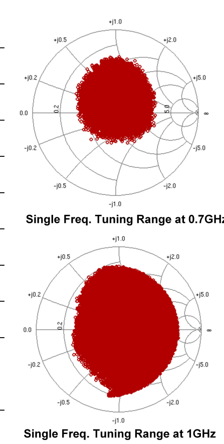

Figure 20.8.6: Performance summary and single-frequency tuning range.

20

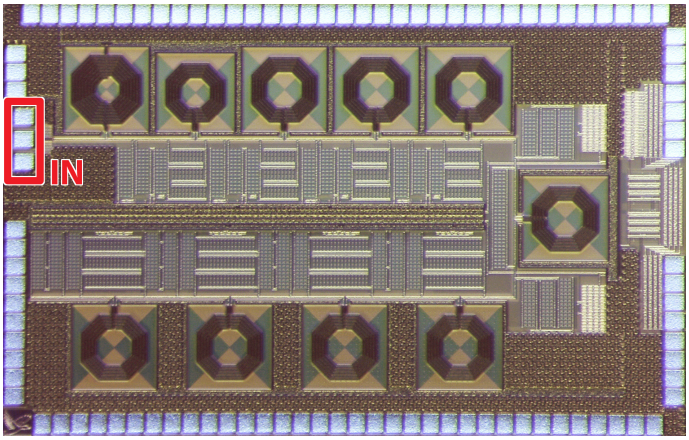

Figure 20.8.7: Die micrograph of the dual-frequency balance network.